

Dynamic Hybrid Position Force Control using Virtual Internal Model to Realize a Cutting Task by a Snake-like Robot

Shunsuke Nansai¹, Mohan Rajesh Elara², and Masami Iwase¹

Abstract—A real snake has simple figure like a string, and has highly adaptability corresponding to the environments/tasks. A snake-like robot mimics such highly adaptability of the real snake, is expected as an adaptable robot corresponding to the environments/tasks. Many literatures have reported with respect to locomotion controls of the snake-like robot, but haven't reported studies for applications. However, enhancement of the applications is required in real scenes of which the snake-like robot is expected to work. This paper reports to design the force controller to realize the cutting task by the snake-like robot, as a leading example of the force control in the real scenes. Since the force control in the feed direction and the servo control in its normal direction are required in order to realize the cutting task, the Dynamic Hybrid Position/Force Control System is designed. The Virtual Internal Model based on the impedance model is utilized as the force control method. The Model Following Servo Control System utilizing the Virtual Internal Model based on the impedance model is designed, and the Dynamic Hybrid Position/Force Control System is realized. Effectiveness of the designed control system is verified through a numerical simulation.

I. INTRODUCTION

A real snake has simple figure like a string, and can locomote by utilizing difference between a friction in the propulsive direction and the one in the normal direction. And it can locomote not only flatland but also desert, wildland and grassland, by choosing its motion and posture depending on environments/tasks. In addition, it can realize skilled locomotions such as swimming, climbing, and squeezing. That is, the real snake has highly adaptability corresponding to the environments/tasks. A snake-like robot mimics such highly adaptability of the real snake, is expected as an adaptable robot corresponding to the environments/tasks.

Many literatures have reported with respect to locomotion controls of the snake-like robot. Hirose, who is a pioneer of the studies for the snake-like robot, has found that a curvature of the snake changes sinusoidally along body axis. And has named it "Serpentoid Curve", and applied to a trajectory generation for the snake-like robot [1]. Endo et al. has implemented a propulsive locomotion control of the snake-like robot by utilizing the "Serpentoid Curve" [2]. As studies applying the "Serpentoid Curve", Yamada et al. [3] and Ma et al. [4] have implemented the stabilization control of a head direction of the robot, and slope climbing control

respectively. Also, we have proposed the tracking control with rotational elastic actuators in our previous study [5]. In addition, a locomotion control utilizing the difference of the friction like the real snake have been proposed. Date et al. [6], Yamakita et al. [7], and Matsuno et al. [8] have implemented the locomotion control avoiding the singular configuration based on the dynamic manipulability by regarding the friction in the normal direction as a constraint force. Inoue et al. have calculated optimal winding angle corresponding to the friction force of the ground [9]. We also have implemented a position control without reference trajectory in our previous study [10], [11]. Whereas these literatures have supposed the unique friction on the ground, Liljeback et al. has implemented a locomotion control utilizing obstacles [12], [13]. Alternatively, locomotions in the 3-dimensional space have proposed. Takayama et al. has developed an amphibious snake-like robot, and has implemented the locomotion control on the ground as well as in the water [14]. Tanaka et al. has proposed the tracking control avoiding slip drop on a cylindrical surface [15]. Thus, many studies for the locomotion control has been reported. On the other hand, studies for applications has been reported only a few. However, enhancement of the applications is required in real scenes, which are expected to be worked by the snake-like robots, such as the forest preservation, the rescues, and the building maintenance. Such scenes require tasks which are applied forces by the robot such as branch cutting, obstacle exclusion, and hammering test. —i.e. the force control is required. For example, Tanaka et al. has realized cooperative control utilizing a number of snake-like robots [16], [17]. This application has realized a force control for transportation. In addition to this application, cutting-tasks including pruning at high-place is expected as applications of the snake-like robot.

This paper reports to design the force controller to realize the cutting task by the snake-like robot, as a leading example of the force control in the real scenes. The cutting task can fall into following three tasks: first task is "touching a saw on an object". Second one is "press the saw continuously". Third one is "stop the saw once cutting is finished". And, this paper addresses the second task "press the saw continuously". In order to realize the cutting task, the force control in the feed direction and the servo control in its normal direction are required. For the effective control system for such task, the Dynamic Hybrid Position/Force Control System [18], [19] erected by Yoshikawa is famous. If the robot outputs too much force to the object, it cannot realized the appropriate cutting because the saw bite the object and/or the saw/object

¹Department of Robotics and Mechatronics, School of Science and Technology for Future Life, Tokyo Denki University, 5 Senjuasahicho, Adachi, Tokyo 120-8551, Japan {nansai, iwase}@ctrl.frc.dendai.ac.jp

²Engineering Product Development Pillar, Singapore University of Technology and Design, 8 Somapah Rd Singapore 487372 rajeshelara@sutd.edu.sg

is broken. In this paper, the Virtual Internal Model [20] based on the impedance model is utilized as the force control method. Hence, a servo controller corresponding to a modified trajectory which is based on the Virtual Internal Model in the feed direction and a reference trajectory in its normal direction is designed. In particular, since the Virtual Internal Model and the reference trajectory can be regarded as a reference model, the Model Following Servo Control System [21] is designed. The Model Following Servo Control System is applied to the snake-like robot, one of nonlinear system, based on the State Dependant Riccati Equation (SDRE) [22], [23], because it is for a linear system.

This paper is organized as follows: In Section II, a dynamic model 8-link snake-like robot is derived. The Model Following Servo Control System based on SDRE is designed in Section III. Section IV verifies an effectiveness of the designed control system through a numerical simulation. Section V concludes this paper.

II. MODELING OF 8-LINK SNAKE-LIKE ROBOT

This section derives the dynamic model of the 8-link snake-like robot by utilizing Projection Method [24], [25], [26]. A schematic figure of the 8-link snake-like robot is shown in Fig. 1 and its physical parameters are shown in Table I. The 8-link snake-like robot addressed in this paper installs a rim saw into a head link, and consists of following two unit: Initial three links are named ‘‘Arm Unit’’, and are utilized for handling the rim saw. Last five links are named ‘‘Snake Unit’’, and are utilized for locomotion. The Snake Unit installs a passive wheel for side slip prevention on the COG of each link. On the other hand, the Arm Unit doesn’t install it to handle the rim saw arbitrarily. $\theta_i(i = 1, \dots, 8)$ represents the absolute angle of i -th link,

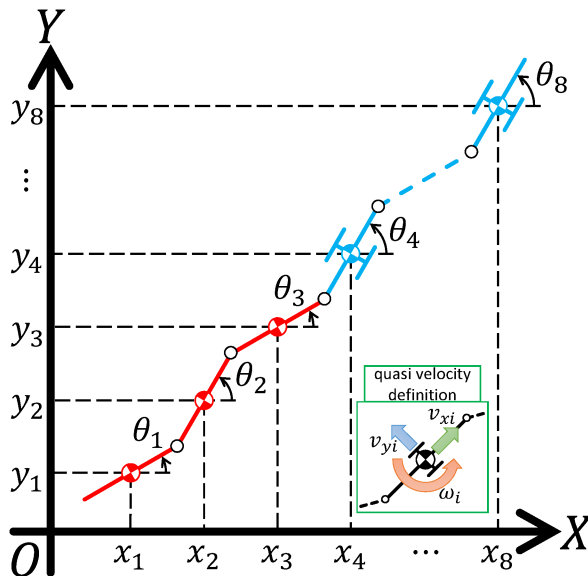


Fig. 1. Schematic figure of the 8-link snake-like robot. Initial three links highlighted in red color are called ‘‘Arm Unit’’ and utilized to manipulate a rim saw. Last five links highlighted in blue color are called ‘‘Snake Unit’’ and utilized for locomotion.

$(x_i, y_i)(i = 1, \dots, 8)$ represents the absolute coordinate of the COG of i -th link, respectively. And, the quasi-velocity is defined on the COG of each link. Firstly, a model of constraint free system is derived. From Fig. 1, the generalized coordinate \mathbf{x}_p of this system is defined as follows.

$$\mathbf{x}_p = [\mathbf{x}_{p1}^T \ \cdots \ \mathbf{x}_{pn}^T]^T, \quad (1)$$

$$\mathbf{x}_{pi} = [\theta_i \ x_i \ y_i]^T, \quad i = 1, \dots, 8.$$

Since to derive the model of the constraint free system means to formulate motion equations both in the rotational direction and in the translation direction of (1), the model of it is derived as follows.

$$\mathbf{M}_p \ddot{\mathbf{x}}_p = \mathbf{h}_p, \quad (2)$$

where, \mathbf{M}_p , \mathbf{h}_p represent the generalized mass matrix and the generalized force matrix respectively, and are defined as follows.

$$\mathbf{M}_p = \text{diag}(\mathbf{M}_{p1}, \dots, \mathbf{M}_{p8}),$$

$$\mathbf{h}_p = [\mathbf{h}_{p1}^T \ \cdots \ \mathbf{h}_{p8}^T]^T,$$

$$\mathbf{M}_{pi} = \text{diag}(J_i, m_i, m_i), \quad i = 1, \dots, 8,$$

$$\mathbf{h}_{pi} = \begin{bmatrix} \tau_i - \tau_{i+1} - C_i(\dot{\theta}_i - \dot{\theta}_{i-1}) + C_{i+1}(\dot{\theta}_{i+1} - \dot{\theta}_i) \\ 0 \\ 0 \end{bmatrix}.$$

$\tau_i(i = 1, \dots, n)$ is defined as input torques into each joint, $\tau_1 = \tau_9 = 0$ and $C_1 = C_9 = 0$ from Fig. 1. The quasi-velocity \mathbf{v} is defined as follows.

$$\mathbf{v}_p = [\mathbf{v}_1^T \ \cdots \ \mathbf{v}_n^T]^T,$$

$$\mathbf{v}_i = [\omega_i \ v_{xi} \ v_{yi}]^T, \quad i = 1, \dots, n.$$

From Fig. 1, the velocity transformation matrix \mathbf{A} relates \mathbf{x}_p and \mathbf{v} as follows.

$$\dot{\mathbf{x}}_p = \mathbf{Av}, \quad (3)$$

$$\mathbf{A} = \text{diag}(\mathbf{A}_1, \dots, \mathbf{A}_8),$$

$$\mathbf{A}_i = \begin{bmatrix} 1 & 0 & 0 \\ 0 & \cos \theta_i & -\sin \theta_i \\ 0 & \sin \theta_i & \cos \theta_i \end{bmatrix}, \quad i = 1, \dots, 8.$$

By (3), (2) is transformed as,

$$\mathbf{M}\dot{\mathbf{v}} = \mathbf{h}, \quad (4)$$

where, $\mathbf{M} = \mathbf{A}^T \mathbf{M}_p \mathbf{A}$, $\mathbf{h} = \mathbf{A}^T (\mathbf{h}_p - \mathbf{M}_p \dot{\mathbf{A}} \mathbf{v})$.

Secondly, a constraint matrix \mathbf{C} of the system satisfying $\mathbf{C}\mathbf{v} = 0$ is derived. From Fig. 1, the robot has two constraint

TABLE I
PHYSICAL PARAMETERS($i = 1, \dots, 8$)

Parameters	Notation	Value
Inertia moment [$\text{kg}\cdot\text{m}^2$]	J_i	0.01
Viscous friction coefficient [$\text{Nm}\cdot\text{s}/\text{rad}$]	C_i	0.001
Mass [kg]	m_i	0.1
Length from center of gravity (COG) to end [m]	l_i	0.1
Length from extremity to COG [m]	d_i	0.1

conditions: every link are connected, and the passive wheel doesn't side slip. With respect to positions of the COG, a holonomic constraint is formulated as,

$$\Phi_h = \begin{bmatrix} x_2 - x_1 - l_1 \cos \theta_1 - d_2 \cos \theta_2 \\ y_2 - y_1 - l_1 \sin \theta_1 - d_2 \sin \theta_2 \\ \vdots \\ x_8 - x_7 - l_7 \cos \theta_7 - d_8 \cos \theta_8 \\ y_8 - y_7 - l_7 \sin \theta_7 - d_8 \sin \theta_8 \end{bmatrix} = 0.$$

From the constraint matrix of which the passive wheel doesn't side slip, with noting that the wheel is installed after 4th link, a nonholonomic constraint is formulated as,

$$\Phi_{nh} = [v_{y4} \quad \dots \quad v_{y8}]^T = 0.$$

By the holonomic/nonholonomic constraint, the constraint matrix of the system is defined as,

$$\begin{aligned} C &= \begin{bmatrix} C_h \\ C_{nh} \end{bmatrix}, \\ C_h &= \frac{\partial \Phi_h}{\partial \mathbf{x}_p} A, \quad C_{nh} = \frac{\partial \Phi_{nh}}{\partial \mathbf{v}}. \end{aligned} \quad (5)$$

Using (5), the model of the constrained system is derived as,

$$M\dot{\mathbf{v}} = \mathbf{h} + C^T \boldsymbol{\lambda}, \quad (6)$$

where, $\boldsymbol{\lambda}$ represents the Lagrange's multipliers.

Finally, (6) is projected into the tangent speed space, and the dynamic model is obtained. From (1), the constraint free system has 24 DOF. From (5), the system is constrained by 14 holonomic constraints and 5 nonholonomic constraints. Hence, the constrained system has 5 DOF. The tangent speed is defined as,

$$\dot{\mathbf{q}} = [\omega_1 \quad v_{x1} \quad v_{y1} \quad \omega_4 \quad v_{x4}]^T.$$

And, replace the quasi-velocity so that satisfying $\mathbf{v}' = [\dot{\mathbf{q}}^T, \mathbf{v}_q^T]^T$, where \mathbf{v}_q represents the dependant velocities with respect to $\dot{\mathbf{q}}$. Also, the constraint matrix C is decomposed into $C = [C_1, C_2]$ satisfying $C\mathbf{v}' = C_1\dot{\mathbf{q}} + C_2\mathbf{v}_q = 0$. The complementary orthogonal matrix D satisfying both $CD = 0$ and $\mathbf{v} = D\dot{\mathbf{q}}$ is derived as

$$D = \begin{bmatrix} I^{5 \times 5} \\ -C_2^{-1}C_1 \end{bmatrix},$$

where, $I^{m \times n}$ represents the identity matrix with $m \times n$. (6) is projected into the tangent speed space by the derived complementary orthogonal matrix D , and we obtain the dynamic model of the system as follows.

$$D^T M D \ddot{\mathbf{q}} + D^T M \dot{D} \dot{\mathbf{q}} = D^T \mathbf{h}. \quad (7)$$

III. CONTROL SYSTEM DESIGN

The Model Following Servo Control system utilizing the Virtual Internal Model based on the impedance model is designed to realize the Dynamic Hybrid Position/Force Control. This paper designs the control system realizing the task "press the saw continuously". The saw should touch the object vertically in order to realize the task. Thus, the attitude of the head has to be controlled as well as the head position.

Since the arm unit has limited operating range, the robot has to locomote to enable to keep its range enough. Hence, the head position of the Snake Unit is controlled to keep a constant distance from the head of the Arm Unit. —i.e., the position and the attitude of the head of the Arm Unit, and the relative distance from the head of the Snake Unit to the one of the Arm Unit are states of the control system. This paper supposes that the object is set parallelly against the y -axis, and a cutting surface moves on the x -axis with minus direction. —i.e., the reference trajectory of the head position decreases on the x -axis from the origin depending on time.

Firstly, a state space representation of the plant model is formulated from (7). The generalized force matrix \mathbf{h} is resolved as,

$$\mathbf{h} = E\mathbf{u} + F\dot{\boldsymbol{\theta}},$$

where,

$$\mathbf{u} = [\tau_2 \quad \dots \quad \tau_8]^T, \quad \dot{\boldsymbol{\theta}} = [\dot{\theta}_1 \quad \dots \quad \dot{\theta}_8]^T,$$

and,

$$E = \frac{\partial \mathbf{h}}{\partial \mathbf{u}}, \quad F = \frac{\partial \mathbf{h} - E\mathbf{u}}{\partial \dot{\boldsymbol{\theta}}}.$$

Since $\mathbf{v} = D\dot{\mathbf{q}}$, H satisfying $\dot{\boldsymbol{\theta}} = H\dot{\mathbf{q}}$ is follows.

$$\begin{aligned} H &= [H_1^T \quad \dots \quad H_8^T]^T, \\ H_i &= D(3i-2), \quad i = 1, \dots, 8, \end{aligned}$$

where, $D(3i-2)$ represents $(3i-2)$ -th row vector of the complementary orthogonal matrix D . And, (7) is transformed as,

$$D^T M D \ddot{\mathbf{q}} + D^T (M \dot{D} - F H) \dot{\mathbf{q}} = D^T E \mathbf{u}.$$

Let the state of the plant model \mathbf{x}_p is $\mathbf{x}_p = \dot{\mathbf{q}}$, and we obtain,

$$\begin{aligned} \dot{\mathbf{x}}_p &= A_p(\mathbf{x}_p)\mathbf{x}_p + B(\mathbf{x}_p)\mathbf{u}, \\ A_p(\mathbf{x}_p) &= (D^T M D)^{-1} D^T (F H - M \dot{D}), \\ B_p(\mathbf{x}_p) &= (D^T M D)^{-1} D^T E \mathbf{u}. \end{aligned} \quad (8)$$

Also, let the output of the plant model is,

$$\mathbf{y} = [\theta_1 \quad x_h \quad y_h \quad x_s - x_h \quad y_s]^T,$$

its output equation is formulated as follows.

$$\begin{aligned} \dot{\mathbf{y}}_p &= C_p \mathbf{x}_p, \\ C_p &= \begin{bmatrix} 1 & 0 & 0 & 0 & 0 \\ d_1 \sin \theta_1 & \cos \theta_1 & -\sin \theta_1 & 0 & 0 \\ -d_1 \cos \theta_1 & \sin \theta_1 & \cos \theta_1 & 0 & 0 \\ -d_1 \sin \theta_1 & -\cos \theta_1 & \sin \theta_1 & d_4 \sin \theta_4 & \cos \theta_4 \\ 0 & 0 & 0 & -d_4 \cos \theta_4 & \sin \theta_4 \end{bmatrix}, \end{aligned} \quad (9)$$

where, x_h , y_h , x_s , y_s represent the x - and y -coordinate of the head position of the robot and the ones of the head position of the snake unit, respectively.

Secondly, a state space representation of the reference model is formulated. The Virtual Internal Model based on the impedance model and the reference trajectory is utilized as the reference model. The impedance model and the reference

trajectory model is constructed in the feed direction (x -axis direction) and its normal direction (y -axis direction) respectively.

$$\begin{aligned}\dot{\mathbf{x}}_r &= \mathbf{A}_r \mathbf{x}_r + \mathbf{B}_r \mathbf{u}_r, \\ \mathbf{x}_r &= \begin{bmatrix} \mathbf{x}_m \\ \dot{\mathbf{x}}_m \end{bmatrix}, \quad \mathbf{A}_r = \begin{bmatrix} \mathbf{0} & \mathbf{I}^{5 \times 5} \\ \mathbf{0} & \mathbf{0} \end{bmatrix}, \quad \mathbf{B}_r = \begin{bmatrix} \mathbf{0} \\ \mathbf{I}^{5 \times 5} \end{bmatrix}.\end{aligned}\quad (10)$$

The input to the reference model \mathbf{u}_r is,

$$\begin{aligned}\mathbf{u}_r &= \ddot{\mathbf{r}}(t) - \mathbf{M}_m^{-1} \mathbf{D}_m (\dot{\mathbf{x}}_m - \dot{\mathbf{r}}(t)) \\ &\quad - \mathbf{M}_m^{-1} \mathbf{K}_m (\mathbf{x}_m - \mathbf{r}(t)) + \mathbf{M}_m^{-1} \mathbf{W} (\mathbf{f} - \mathbf{f}_d),\end{aligned}$$

$$\mathbf{M}_m = \text{diag}(m_{m1}, m_{m2}, m_{m3}, m_{m4}, m_{m5}),$$

$$\mathbf{D}_m = \text{diag}(0, d_{m2}, 0, d_{m4}, 0),$$

$$\mathbf{K}_m = \text{diag}(0, k_{m2}, 0, k_{m4}, 0),$$

$$\mathbf{W} = \begin{bmatrix} 0 & 1 & 0 & -1 & 0 \\ 0 & 0 & 0 & 0 & 0 \end{bmatrix}^T,$$

where, \mathbf{M}_m , \mathbf{D}_m , \mathbf{K}_m represent the mass, the damping coefficient, and the elastic coefficient of the impedance model. And, \mathbf{f} , \mathbf{f}_d represent a disturbance with a reaction force from the object, and a target force (Fig. 2). A output equation of the reference model is defined as follows.

$$\begin{aligned}\dot{\mathbf{y}}_r &= \mathbf{C}_r \mathbf{x}_r, \\ \mathbf{C}_r &= [\mathbf{0} \quad \mathbf{I}^{5 \times 5}].\end{aligned}\quad (11)$$

We define an error between the plant model and the reference model as,

$$\mathbf{e}' = \mathbf{y}_p - \mathbf{y}_r,$$

The error system is modeled as,

$$\dot{\mathbf{e}} = \begin{bmatrix} \mathbf{e}' \\ \dot{\mathbf{e}}' \end{bmatrix} = \begin{bmatrix} \mathbf{0} & \mathbf{I}^{5 \times 5} \\ \mathbf{0} & \mathbf{0} \end{bmatrix} \mathbf{e}. \quad (12)$$

By regarding that (8) and (9) are linear time-invariant system within the sampling interval, an augmented system shown in (13) is obtained from (8), (10), (12).

$$\dot{\xi} = \bar{\mathbf{A}}\xi + \bar{\mathbf{B}}\dot{\mathbf{u}}_p, \quad (13)$$

where, $\xi = [\dot{\mathbf{x}}_p^T \quad \mathbf{e}^T \quad \dot{\mathbf{x}}_r^T]^T$, and,

$$\bar{\mathbf{A}} = \begin{bmatrix} \mathbf{A}_p(\mathbf{x}_r) & \mathbf{0} & \mathbf{0} & \mathbf{0} \\ \mathbf{0} & \mathbf{0} & \mathbf{I} & \mathbf{0} \\ \mathbf{C}_p & \mathbf{0} & \mathbf{0} & -\mathbf{C}_r \\ \mathbf{0} & \mathbf{0} & \mathbf{0} & \mathbf{A}_r \end{bmatrix}, \quad \bar{\mathbf{B}} = \begin{bmatrix} \mathbf{B}_p(\mathbf{x}_p) \\ \mathbf{0} \\ \mathbf{0} \\ \mathbf{0} \end{bmatrix}.$$

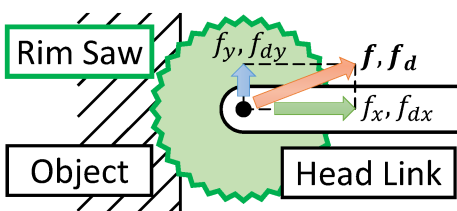


Fig. 2. The disturbance with the reaction force from the object \mathbf{f} , and the target force \mathbf{f}_d .

Now, we consider a criterion function shown in (14) for (13).

$$J = \int_0^\infty (\mathbf{e} \mathbf{Q}(\xi) \mathbf{e} + \mathbf{u}_p^T \mathbf{R}(\xi) \mathbf{u}_p) dt, \quad (14)$$

where, $\mathbf{Q}(\xi)$ and $\mathbf{R}(\xi)$ represent weighting matrices with respect to the error and the input, and are chosen as semi-positive definite and positive definite respectively. The control input \mathbf{u}_p minimizing (14) is obtained as,

$$\mathbf{u}_p = \mathbf{F}_1 \mathbf{x}_p + \mathbf{F}_2 \int_0^t \mathbf{e} d\tau + \mathbf{F}_3 \mathbf{x}_r,$$

with feedback gains \mathbf{F}_1 , \mathbf{F}_2 , and \mathbf{F}_3 . These gains are given as follows.

$$\begin{aligned}[\mathbf{F}_1 \quad \mathbf{F}_2] &= -\mathbf{R}(\xi)^{-1} \mathbf{B}_1(\xi)^T \mathbf{P}_{11}(\xi), \\ \mathbf{F}_3 &= -\mathbf{R}(\xi)^{-1} \mathbf{B}_1(\xi)^T \mathbf{P}_{12}(\xi),\end{aligned}$$

where, $\mathbf{P}_{11}(\xi)$ is a symmetric positive definite matrix which is solution of SDRE shown as follows.

$$\begin{aligned}\mathbf{A}_1^T(\xi) \mathbf{P}_{11}(\xi) + \mathbf{P}_{11}(\xi) \mathbf{A}_1(\xi) + \mathbf{Q}_1(\xi) \\ - \mathbf{P}_{11}(\xi) \mathbf{B}_1(\xi) \mathbf{R}(\xi)^{-1} \mathbf{B}_1(\xi)^T \mathbf{P}_{11}(\xi) = 0,\end{aligned}$$

where,

$$\begin{aligned}\mathbf{A}_1(\xi) &= \begin{bmatrix} \mathbf{A}_p(\mathbf{x}_r) & \mathbf{0} & \mathbf{0} \\ \mathbf{0} & \mathbf{0} & \mathbf{I} \\ \mathbf{C}_p & \mathbf{0} & \mathbf{0} \end{bmatrix}, \quad \mathbf{B}_1(\xi) = \begin{bmatrix} \mathbf{B}_p(\mathbf{x}_p) \\ \mathbf{0} \\ \mathbf{0} \end{bmatrix}, \\ \mathbf{Q}_1(\xi) &= \begin{bmatrix} \mathbf{0} & \mathbf{0} \\ \mathbf{0} & \mathbf{Q}(\xi) \end{bmatrix}.\end{aligned}$$

And, $\mathbf{P}_{11}(\xi)$ is a solution of a following algebraic equation.

$$\begin{aligned}\mathbf{A}_1^T(\xi) \mathbf{P}_{12}(\xi) + \mathbf{P}_{12}(\xi) \mathbf{A}_2 + \mathbf{P}_{12}(\xi) \mathbf{A}_r \\ - \mathbf{P}_{11}(\xi) \mathbf{B}_1(\xi) \mathbf{R}(\xi)^{-1} \mathbf{B}_1(\xi)^T \mathbf{P}_{12}(\xi) = 0.\end{aligned}$$

where,

$$\mathbf{A}_2 = [\mathbf{0} \quad \mathbf{0} \quad -\mathbf{C}_r^T]^T.$$

IV. NUMERICAL SIMULATION

This section verifies effectiveness of the control system designed in Section III through a numerical simulation. MaTX (Visual C++ 2012 version 5.3.45) [27] is performed for the simulation. The simulation parameters are shown in Table I. A simulation time and a sampling interval were 20 s, and 0.01 s, and the ordinary differential equation was solved by the function “rkf45”. Initial conditions of the robot were with $\theta_1 = 0$ rad, $\theta_2 = -\pi/6$ rad, $\theta_3 = \pi/6$ rad, $\theta_i = 0.5 \cos(-(i-4)\pi/6.0)$, ($i = 4, \dots, 8$) rad. The target force \mathbf{f}_d for cutting was set as,

$$\mathbf{f}_d = [f_{dx} \quad f_{dy}]^T = [1 \quad 0]^T.$$

Generally, the reaction force from the object include noises. The noises including the reaction force are generated as,

$$\mathbf{f} = \begin{bmatrix} f_x \\ f_y \end{bmatrix} = \begin{bmatrix} 0.5 & 0 \\ 0 & 0.1 \end{bmatrix} \mathbf{f}_{nr} + \mathbf{f}_d,$$

by utilizing normal random numbers \mathbf{f}_{nr} , where, \mathbf{f}_{nr} are generated by a function “randn”. And, based on the virtual

work principle, forces generated by the robot \bar{f} are derived as follows.

$$\bar{f} = J^T D^T E u = C_p^T D^T E u.$$

The reference trajectory $r(t)$ was,

$$r(t) = \begin{cases} r_1(t), & (t \leq 1), \\ r_2(t), & (t > 1), \end{cases}$$

$$r_1(t) = \begin{bmatrix} 0 \\ -0.125t^4 \\ \sum_{i=1}^3 (d_i + l_i) \cos \theta_i(0) \\ 0 \end{bmatrix},$$

$$r_2(t) = \begin{bmatrix} 0 \\ -0.5t + 0.375 \\ \sum_{i=1}^3 (d_i + l_i) \cos \theta_i(0) \\ 0 \end{bmatrix},$$

where, $\theta_i(0)$ represents the initial angle of θ_i . The parameters of the impedance model were,

$$M_m = \text{diag}(0.3, 0.3, 0.3, 0.3, 0.3),$$

$$D_m = \text{diag}(0, 0.5, 0, 0.5, 0),$$

$$K_m = \text{diag}(0, 10, 0, 10, 0),$$

and, the weighting matrices Q , R were,

$$Q = \text{diag}(0.001 \times I(4), 0.1, 1000 \times I(4), 0.1),$$

$$R = 10 \times I(7).$$

Simulation results are shown in Figs. 3-9. From Fig. 3, tau $\tau_5 \sim \tau_8$, that is, the input torques of the Snake Unit are output sinusoidally with almost same phase-lag. It are found commonly when realizing a serpentine locomotion which is characteristic of the real snake. Thus, the robot locomotes with generating the serpentine locomotion by the designed control system. Fig. 4 shows that θ_1 tracks to the reference trajectory within 10^{-3} order, even though the head is gotten the reaction force including the noises shown in Fig. 8. Fig. 6 also shows that y_h tracks within 10^{-2} th

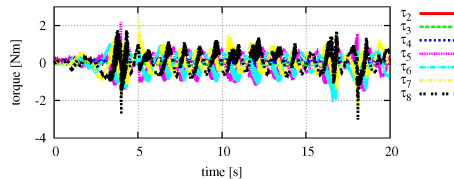


Fig. 3. Time variant of the input torques.

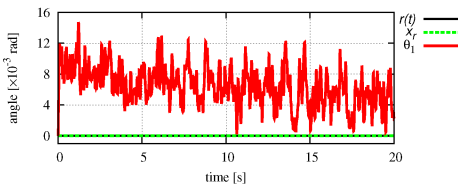


Fig. 4. Time variant of θ_1 , the reference trajectory and x_r for θ_1 .

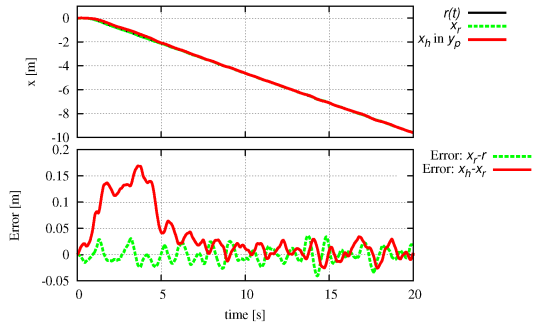


Fig. 5. Time variant of x_h , the reference trajectory and x_r for x_h (**Top**). Time variant of errors between x_h and x_r , and the reference trajectory and x_r (**Bottom**).

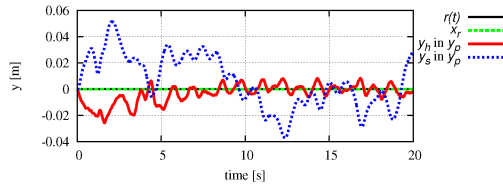


Fig. 6. Time variant of y_h , y_s , the reference trajectory and x_r for y_h .

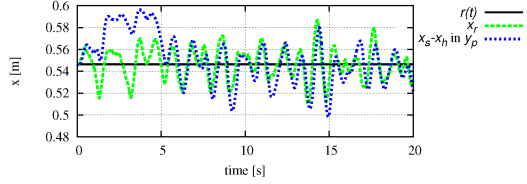


Fig. 7. Time variant of $x_s - x_h$, the reference trajectory and x_r for $x_s - x_h$.

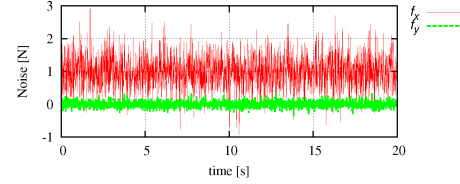


Fig. 8. Time variant of the reaction force f with the noises.

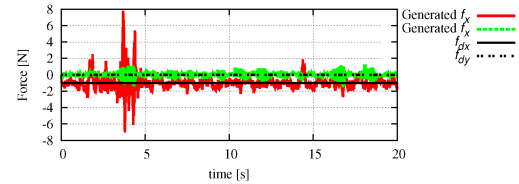


Fig. 9. Time variant of the target force f_d and the force f generated by the robot with the input torques shown in Fig. 3.

order. And, Fig. 4 and Fig. 6 shows that the output of the reference model equals the reference trajectory. Thus, the servo control system tracking to the reference trajectory has been designed in the normal direction of the feed direction. Fig. 5 and Fig. 7 shows that the states of the reference model are changed by the reaction force including the noises shown in Fig. 8. These show that x_h and $x_s - x_h$ tracks to the reference model as well. Thus, the servo control system tracking to the Virtual Internal Model based on the impedance model has been designed in the feed direction.

TABLE II
AVERAGE AND STANDARD DEVIATION OF \bar{f}

Parameters	Average [N]	Standard Deviation [N]
\bar{f}_x	-0.9361	0.8513
\bar{f}_y	0.0087	0.3764

Averages and standard deviations of the actual generated forces shown in Fig. 9 are shown in Table II. Fig 1 and Table 1 shows that the robot generates approximately -1 N in the x -axis (the feed direction) and approximately 0 N in the y -axis (its normal direction). Thus, it is confirmed that the cutting task is realized by the designed Dynamic Hybrid Position/Force Control System through the numerical simulation, because the force control system and the servo control system are designed in the feed direction and its normal direction respectively.

V. CONCLUSION

This paper has aimed to realize the cutting task by the snake-like robot, and designed the Dynamic Hybrid Position/Force Control System utilizing the Virtual Internal Model based on the impedance model. Since a normal snake-like robot cannot realize the cutting task, we have supposed the snake-like robot installing the rim saw on the head. Because it should be handled arbitrarily in order to realize the cutting task, the 8-link snake-like robot has fallen into following two units: Initial three links are the arm unit. Last five links are the snake unit. The arm unit doesn't install the passive wheel to handle the rim saw, but the snake unit installs it on the COG of each link. And, the dynamic model of the robot has been derived by utilizing Projection Method. The Dynamic Hybrid Position/Force Control System utilizing the Virtual Internal Model based on the impedance model realizing the force control in the feed direction and the servo control in its normal direction has been designed. Furthermore, the Model Following Servo Control System based on SDRE has been designed. The effectiveness of the designed control system has been verified through the numerical simulation. As the result, the control system to realize the cutting task by the snake-like robot has been designed.

REFERENCES

- [1] S. Hirose, *Biologically Inspired Robots: Snake-Like Locomotors and Manipulators*. Oxford University Press, 1993.
- [2] G. Endo, K. Togawa, and S. Hirose, "Study on self-contained and terrain adaptive active cord mechanism," in *Intelligent Robots and Systems, 1999. IROS'99. Proceedings. 1999 IEEE/RSJ International Conference on*, vol. 3. IEEE, 1999, pp. 1399–1405.
- [3] H. Yamada, M. Mori, and S. Hirose, "Stabilization of the head of an undulating snake-like robot," in *Intelligent Robots and Systems, 2007. IROS 2007. IEEE/RSJ International Conference on*. IEEE, 2007, pp. 3566–3571.
- [4] S. Ma and N. Tadokoro, "Analysis of creeping locomotion of a snake-like robot on a slope," *Autonomous Robots*, vol. 20, no. 1, pp. 15–23, 2006.
- [5] S. Nansai and M. Iwase, "Tracking control of snake-like robot with rotational elastic actuators," in *Control, Automation and Systems (ICCAS), 2012 12th International Conference on*, 2012, pp. 678–683.
- [6] H. Date, Y. Hoshi, and M. Sampei, "Locomotion control of a snake-like robot based on dynamic manipulability," in *Intelligent Robots and Systems, 2000.(IROS 2000). Proceedings. 2000 IEEE/RSJ International Conference on*, vol. 3, 2000, pp. 2236–2241.
- [7] M. Yamakita, M. Hashimoto, and T. Yamada, "Control of locomotion and head configuration of 3d snake robot (sma)," in *Robotics and Automation, 2003. Proceedings. ICRA'03. IEEE International Conference on*, vol. 2. IEEE, 2003, pp. 2055–2060.
- [8] F. Matsuno and H. Sato, "Trajectory tracking control of snake robots based on dynamic model," in *Robotics and Automation, 2005. ICRA 2005. Proceedings of the 2005 IEEE International Conference on*, 2005, pp. 3029–3034.
- [9] I. Koussuke, S. Takaaki, and S. Ma, "Cpg-based control of a simulated snake-like robot adaptable to changing ground friction," in *2007 IEEE/RSJ International Conference on Intelligent Robots and Systems*, 2007, pp. 1957–1962.
- [10] K. Watanabe, M. Iwase, S. Hatakeyama, and T. Maruyama, "Control strategy for a snake-like robot based on constraint force and its validation," in *Advanced intelligent mechatronics, 2007 IEEE/ASME international conference on*, 2007, pp. 1–6.
- [11] K. Watanabe, M. Iwase, S. Hatakeyama, and T. Maruyama, "Control strategy for a snake-like robot based on constraint force and verification by experiment," *Advanced Robotics*, vol. 23, no. 7-8, pp. 907–937, 2009.
- [12] A. A. Transeth, R. Leine, C. Glocker, K. Y. Pettersen, and P. Liljeback, "Snake robot obstacle-aided locomotion: Modeling, simulations, and experiments," *Robotics, IEEE Transactions on*, vol. 24, no. 1, pp. 88–104, 2008.
- [13] P. Liljeback, K. Y. Pettersen, Ø. Stavdahl, and J. T. Gravdahl, "Hybrid modelling and control of obstacle-aided snake robot locomotion," *Robotics, IEEE Transactions on*, vol. 26, no. 5, pp. 781–799, 2010.
- [14] T. Toshio and H. Shigeo, "Amphibious 3d active cord mechanism "helix" with helical swimming motion," in *2002 IEEE/RSJ International Conference on Intelligent Robots and Systems*, 2002, pp. 775–780.
- [15] M. Tanaka, H. Tsukano, and F. Matsuno, "Trajectory tracking control of a snake robot on cylindrical surface with considering avoidance of sliding down," *Transactions of the Society of Instrument and Control Engineers*, vol. 48, pp. 664–673, 2012.
- [16] M. Tanaka and F. Matsuno, "Cooperative control of two snake robots," in *Robotics and Automation, 2006. ICRA 2006. Proceedings 2006 IEEE International Conference on*. IEEE, 2006, pp. 400–405.
- [17] M. Tanaka and F. Matsuno, "Cooperative control of three snake robots," in *Intelligent Robots and Systems, 2006 IEEE/RSJ International Conference on*. IEEE, 2006, pp. 3688–3693.
- [18] T. Yoshikawa, "Dynamic hybrid position/force control of robot manipulators—description of hand constraints and calculation of joint driving force," *Robotics and Automation, IEEE Journal of*, vol. 3, no. 5, pp. 386–392, 1987.
- [19] T. Yoshikawa, T. Sugie, and M. Tanaka, "Dynamic hybrid position/force control of robot manipulators—controller design and experiment," *Robotics and Automation, IEEE Journal of*, vol. 4, no. 6, pp. 699–705, 1988.
- [20] M. Koga, K. Kosuge, K. Furuta, and K. Nosaki, "Coordinated motion control of robot arms based on the virtual internal model," *Robotics and Automation, IEEE Transactions on*, vol. 8, no. 1, pp. 77–85, 1992.
- [21] K. Furuta and K. Komiya, "Design of model-following servo controller," *Automatic Control, IEEE Transactions on*, vol. 27, no. 3, pp. 725–727, 1982.
- [22] J. R. Cloutier, "State-dependent riccati equation techniques: an overview," in *American Control Conference, 1997. Proceedings of the 1997*, no. 2, 1997, pp. 932–936.
- [23] T. Cimen, "State-dependent riccati equation (sdre) control: a survey," in *Proceedings of the 17th World Congress of the International Federation of Automatic Control (IFAC)*, Seoul, Korea, July, 2008, pp. 6–11.
- [24] K. Arczewski and W. Blajer, "A unified approach to the modelling of holonomic and nonholonomic mechanical systems," *mathematical modelling of systems*, vol. 2, no. 3, pp. 157–174, 1996.
- [25] W. Blajer, "A geometrical interpretation and uniform matrix formulation of multibody systems dynamics," *Z. Angew. Math. Mech.*, vol. 81, no. 4, pp. 247–259, 2004.
- [26] H. Ohsaki, M. Iwase, and S. Hatakeyama, "A consideration of nonlinear system modeling using the projection method," in *SICE Annual Conference*, 2007, pp. 1915–1920.
- [27] M. Koga, "Matx/rtmatx: A freeware for integrated cacs," *Proceedings of the 1999 IEEE International Symposium on Computer Aided Control System Design*, pp. 452–456, 1999.